



GE Nuclear Energy

175 Curtner Avenue  
San Jose, CA 95125

NEDC-30634  
Revision 1  
DRF B11-00491  
Class III  
May 1991

GE NUCLEAR ENERGY

BRUNSWICK STEAM ELECTRIC PLANT, UNIT 1  
FEEDWATER NOZZLE FRACTURE MECHANICS ANALYSIS

G. L. Stevens

Approved:

S. Ranganath, Manager  
Materials Monitoring and Structural  
Analysis Services

IMPORTANT NOTICE REGARDING  
CONTENTS OF THIS REPORT  
PLEASE READ CAREFULLY

This report was prepared by the General Electric Company (GE) solely for the use of Carolina Power and Light Company. The information contained in this report is believed by GE to be an accurate and true representation of the facts known, obtained or provided to GE at the time this report was prepared.

The only undertakings of the General Electric Company respecting information in this document are contained in Carolina Power and Light Company Work Authorization No. ZS70020028 and nothing contained in this document shall be construed as changing said contract. The use of this information except as defined by said contract, or for any purpose other than that for which it is intended, is not authorized; and with respect to any such unauthorized use, neither GE nor any of the contributors to this document makes any representation or warranty (express or implied) as to the completeness, accuracy or usefulness of the information contained in this document or that such use of such information may not infringe privately owned rights; nor do they assume any responsibility for liability or damage of any kind which may result from such use of such information.

## CONTENTS

	<u>Page</u>
ABSTRACT	v
1. INTRODUCTION	1-1
1.1 Background	1-1
1.2 Objective	1-1
1.3 Technical Approach	1-2
1.3.1 Feedwater Flow Cycling	1-2
1.3.2 Thermal Cycling	1-2
2. SUMMARY AND CONCLUSIONS	2-1
3. THERMAL CYCLE DEFINITION	3-1
4. THERMAL ANALYSIS	4-1
5. THERMAL AND PRESSURE STRESSES	5-1
6. CRACK GROWTH ANALYSIS	6-1
6.1 Stress Intensity Factor Calculations	6-1
6.2 Crack Growth Data	6-5
6.3 Crack Growth Evaluation	6-5
7. RESULTS AND CONCLUSIONS	7-1
8. REFERENCES	8-1
APPENDIX - THERMAL BOUNDARY CONDITIONS	A-1

## TABLES

<u>Table</u>	<u>Title</u>	<u>Page</u>
5-1	Surface Stresses to Choose Maximum Combined Stresses	5-2
5-2	Limiting Stress Profile (Cross Section 4-4)	5-7

## ILLUSTRATIONS

<u>Figure</u>	<u>Title</u>	<u>Page</u>
3-1	Temperature Cycling for 7/1/87 Scram	3-4
3-2	Temperature Cycling for Planned Shutdown of 1/23/88	3-5
3-3	Temperature Cycling for 5/21/88 Maintenance Shutdown	3-6
3-4	Temperature Cycling for 7/13/88 Forced Shutdown	3-7
3-5	Temperature Cycling for 11/10/88 Refueling Shutdown	3-8
4-1	Nozzle Configuration	4-2
4-2	Thermal Boundary Conditions	4-3
5-1	Feedwater Nozzle-Brunswick 1 Location of Maximum Surface Stress (Steady State)	5-4
5-2	Feedwater Nozzle-Brunswick 1 Location of Maximum Surface Stress (Transient $t = 4$ minutes)	5-5
6-1	Boundary Integral Equation/Influence Function Magnification Factors for BWR Feedwater Nozzle	6-2
6-2	Stress Intensity Factor versus Crack Depth (Thermal Stresses, 4 minutes)	6-3
6-3	Stress Intensity Factor versus Crack Depth (Pressure Stresses)	6-4
6-4	Reference Fatigue Crack Growth Curves for Carbon and Low Alloy Ferritic Steels	6-6
7-1	Crack Depth versus Number of Years	7-2

ABSTRACT

The current revision of this report is based on actual feedwater cycling data collected for Brunswick 1 since the original (July 1984) revision of this report.

This report provides a plant-specific fracture mechanics assessment of the Brunswick 1 feedwater nozzles to show compliance with NUREG-0619 as amended by NRC Generic Letter 81-11, dated February 20, 1981. The evaluation was based upon (1) the plant operating history supplied by Carolina Power and Light Company (CP&L), (2) low feedwater flow characteristics determined from actual plant feedwater cycling measurements, and (3) Moss Landing test data. The evaluation considered an initial crack depth of 0.25 inch as specified in NUREG-0619. The results show that stress cycling from actual temperature and flow profiles results in the growth of an initial 0.25-inch crack to less than 1 inch during the remaining life of the plant. Using the 1989 ASME Section XI fatigue crack growth curves, the analysis shows that the postulated 0.25-in. crack becomes 0.56 inch deep after the 40-year plant design life.

These results demonstrate full compliance of the low flow feedwater controller with the requirements specified in NUREG-0619.

## 1. INTRODUCTION

This report provides a plant-specific feedwater nozzle fracture mechanics assessment based on the Brunswick Steam Electric Plant, Unit 1 (hereafter called Brunswick 1) plant operating history and actual feedwater cycling data. This is in response to the Nuclear Regulatory Commission (NRC) requirements regarding feedwater nozzle crack growth. These requirements are contained in the NRC Generic Letter 81-11 which states that a fracture mechanics evaluation must predict an end-of-design-life crack size of 1 inch or less.

### 1.1 BACKGROUND

The General Electric Company (GE) feedwater nozzle final report (Reference 1) recommended design and operational changes to minimize both the probability of crack initiation and rate of crack growth in feedwater nozzles. The low flow feedwater controller discussed in Reference 1 would not significantly reduce the probability of crack initiation, but would reduce crack growth. The NRC (NUREG-0619) accepted the GE recommendation (Reference 1) and required that operating reactors install a low flow feedwater controller with the characteristics described in Reference 1 and reroute the Reactor Water Cleanup System (RWCS) flow to all of the feedwater lines. The low flow controller required above must meet strict requirements specified in Subsection 3.4.4.3 of Reference 1. The NRC later clarified its position in Generic Letter 81-11, stating that plant-specific analyses may be performed to justify not implementing such modifications.

With respect to low flow feedwater controller installation assessment, feedwater nozzle crack growth rate analysis is required for Brunswick 1.

### 1.2 OBJECTIVE

Because of the absence of Brunswick 1 low flow feedwater controller data, temperature measurement hardware was installed subsequent to the July 1984 revision of this report. The data collected by that hardware for the last

fuel cycle was utilized as a basis for defining the actual Brunswick 1 feedwater cycling characteristics used in the current analysis. The data collected was considered typical for the entire design life of the reactor.

This report provides a plant-specific fracture mechanics assessment of the Brunswick 1 feedwater nozzles to show compliance with the requirements of NUREG-0619 as amended by Generic Letter 81-11, dated February 20, 1981. The purpose of this analysis is to determine whether stress cycling from actual controller temperature and flow fluctuations will result in a final crack depth of 1 inch or less during a 40-year plant design life. The evaluation considers an initial crack depth of 0.25 inch as specified in NUREG-0619.

### 1.3 TECHNICAL APPROACH

This analysis evaluates the growth of a 0.25-inch crack over a projected 40-year plant design life.

#### 1.3.1 Feedwater Flow Cycling

The feedwater flow cycling was determined from actual feedwater temperature and flow data obtained from CP&L (Reference 2).

#### 1.3.2 Thermal Cycling

The thermal cycling of the fluid at the feedwater nozzle was determined from the actual feedwater data. The number of startup/shutdown and scram events for Brunswick 1 was linearly projected based on actual plant operating history during the first 12 years (1976-1988) of plant operation (References 2, 3 and 4).

The thermal boundary conditions used in this analysis differed from the Reference 1 document in that thermal sleeve annulus temperatures and annulus heat transfer coefficients, derived from Moss Landing test data (Reference 9), were used to calculate the thermal stresses in the feedwater nozzle.

To evaluate the crack growth, thermal and pressure stress analyses were conducted using the finite element computer code ANSYS (Reference 6). The locations of the peak thermal stress, peak pressure stress and peak combined thermal and pressure stress were determined and the crack growth was calculated using a crack growth computer code. The crack growth relationship used represents the 1989 ASME Section XI Code Curves. The best-fit correlation to actual PWR and BWR data used in the original revision of this report was not used, since the R-ratios ( $K_{min}/K_{max}$ ) were typically high for the actual cycling data; that correlation is not valid for high R-ratios.



## 2. SUMMARY AND CONCLUSIONS

Application of the ASME Code, Section XI crack growth rate relationship resulted in crack growth less than the acceptance criterion of 1 inch for a 40-year plant life. The analysis resulted in a 0.56-inch crack depth after the 40-year plant design life.

This analysis is based on actual low flow feedwater controller characteristics obtained since the original revision of this report. The plant operating history is based on the initial 12 years of operation extrapolated to 40 years. Because of "learning curve" effects which are typically experienced by operating reactors during their initial years of operation, the extrapolation is most likely conservative.

With regards to RWCU reroute, a plant-specific analysis was performed for Brunswick 1 which demonstrates that RWCU reroute leads to only a small improvement on thermal cycling and fatigue usage of the feedwater nozzle region (Reference 14). Based on that analysis, it was concluded that monitoring thermal sleeve seal is more important than RWCU reroute.

Therefore, based on the results presented herein, it is concluded that the Brunswick 1 low flow controller fully meets the requirements of NUREG-0619. Periodic examination, required by NUREG-0619, of the feedwater nozzle will provide additional justification of these analytical results.

### 3. THERMAL CYCLE DEFINITION

The feedwater nozzle thermal cycle definitions are represented by Figures 3-1 through 3-5. These figures represent the minimum and maximum temperature points for one scram event and several startup/shutdown events obtained from CP&L for Brunswick 1. The feedwater loop which has the RWCS mixing (Loop B) had the most severe cycling and was therefore used throughout this analysis.

The following events appropriate for this analysis were identified by CP&L personnel from the last available fuel cycle:

<u>Figure</u>	<u>Date</u>	<u>Event Description</u>
3-1	7/1/87	Scram
3-2	1/23/88	Planned Shutdown
3-3	5/21/88	Maintenance Shutdown
3-4	7/13/88	Forced Shutdown
3-5	11/10/88	Refueling Shutdown

These events are depicted in Figures 3-1 through 3-5, and were digitized into computer form from microfilmed strip chart recordings of feedwater temperature. The temperature measurements were taken by hardware installed subsequent to the original issue of this report, and are symbolic of the cycling occurring at the feedwater nozzle. The events are shown exactly as digitized from the microfilm recordings; as a consequence, actual progress of each event is from right to left.

A total projection of 163 startup/shutdown events and 323 scram events over the 40-year plant life was made for Brunswick 1 based on operating data obtained from the first 12 years of operation (References 2, 3 and 4). This projection was determined using the methodology of Reference 5 as follows:

<u>Year</u>	<u>Time Period</u>	<u>Number of Startups/Shutdowns</u>	<u>Number of Scrams*</u>
1	11/76 - 11/77	2	29
2	11/77 - 11/78	1	21
3	11/78 - 11/79	5	17
4	11/79 - 11/80	7	10
5	11/80 - 11/81	3	10
6	11/81 - 11/82	5	15
7	11/82 - 11/83	4	7
8	11/83 - 11/84	7	9
9	11/84 - 11/85	3	4
10	11/85 - 11/86	0	8
11	11/86 - 11/87	6	1
12	11/87 - 11/88	5	3
12.5	11/88 - 5/89	2	1

\*Note: Turbine trips identified in Reference 4 were counted as scram events. Although conservative, this method of counting is not considered to be a significant contributor to the final crack growth results.

Based on the methods of Reference 5, the following equation is used to determine the projected number of events for the 40-year design life:

$$n_{40} = n_4 + n_{12.5} [36 / (12.5 - 4)]$$

where  $n_{40}$  = projected number of events at year 40  
 $n_4$  = number of events at year 4  
 $n_{12.5}$  = number of events between year 4 and year 12.5

Thus, for startup/shutdown events, the following is obtained:

$$n_{40} = 15 + 35(36/8.5) = 163$$

and for scram events:

$$n_{40} = 77 + 58(36/8.5) = 323$$

For the purposes of this analysis, a single cycle is defined when the nozzle fluid temperature, initially at some value  $T_0$ , changes to some other value  $T_1$  and then returns to  $T_0$ .

For the purposes of defining complete startup/shutdown cycles, the start-ups corresponding to each of the four shutdown events (Figures 3-2 through 3-5) were assumed to be mirror images (i.e., identical) to the shutdown events. Therefore, four (4) complete startup/shutdown cycles and one (1) complete scram cycle define the thermal cyclic duty experienced by Brunswick 1. These events were assumed to be typical for the entire 40-year design life of the reactor.

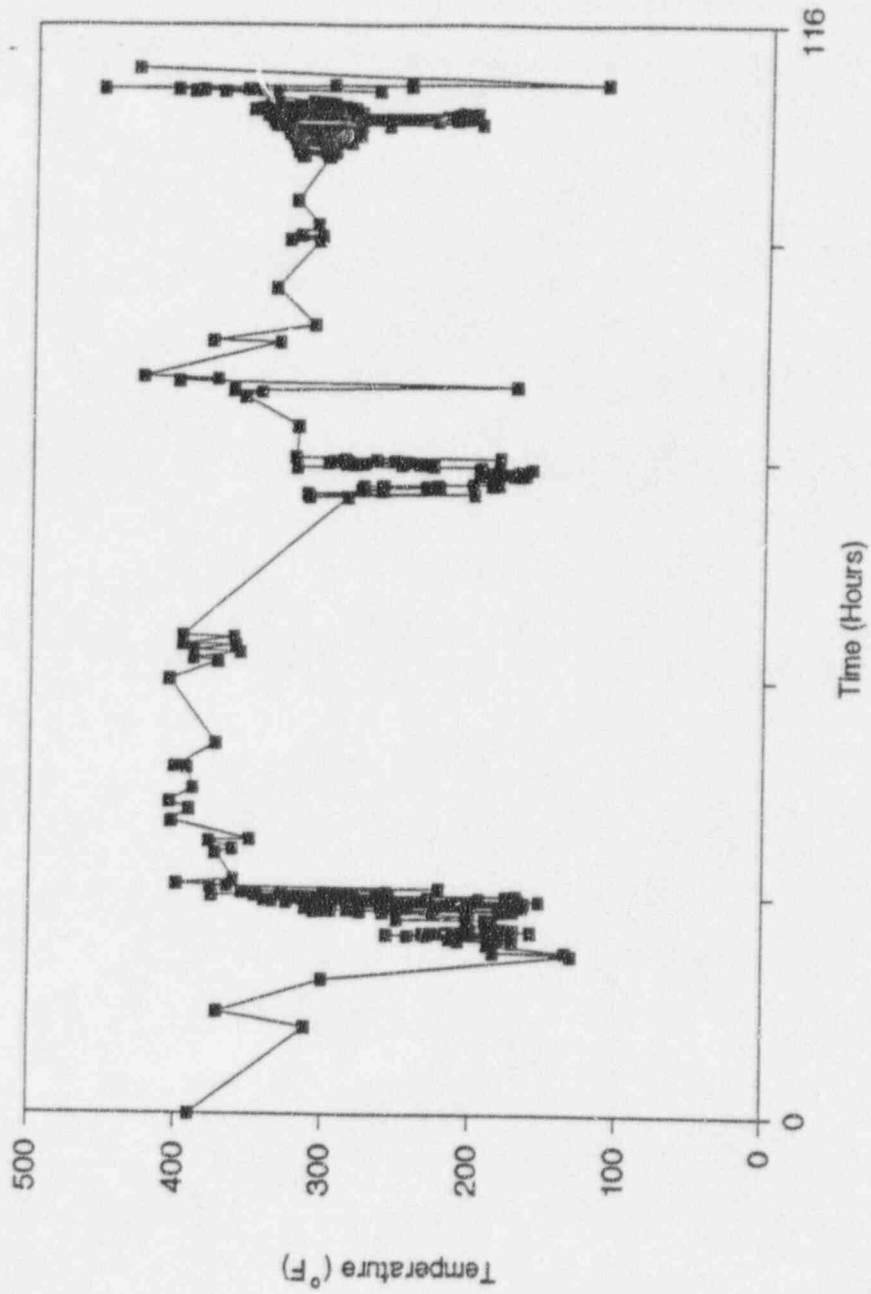


Figure 3-1. Temperature Cycling for 7/1/87 Scram

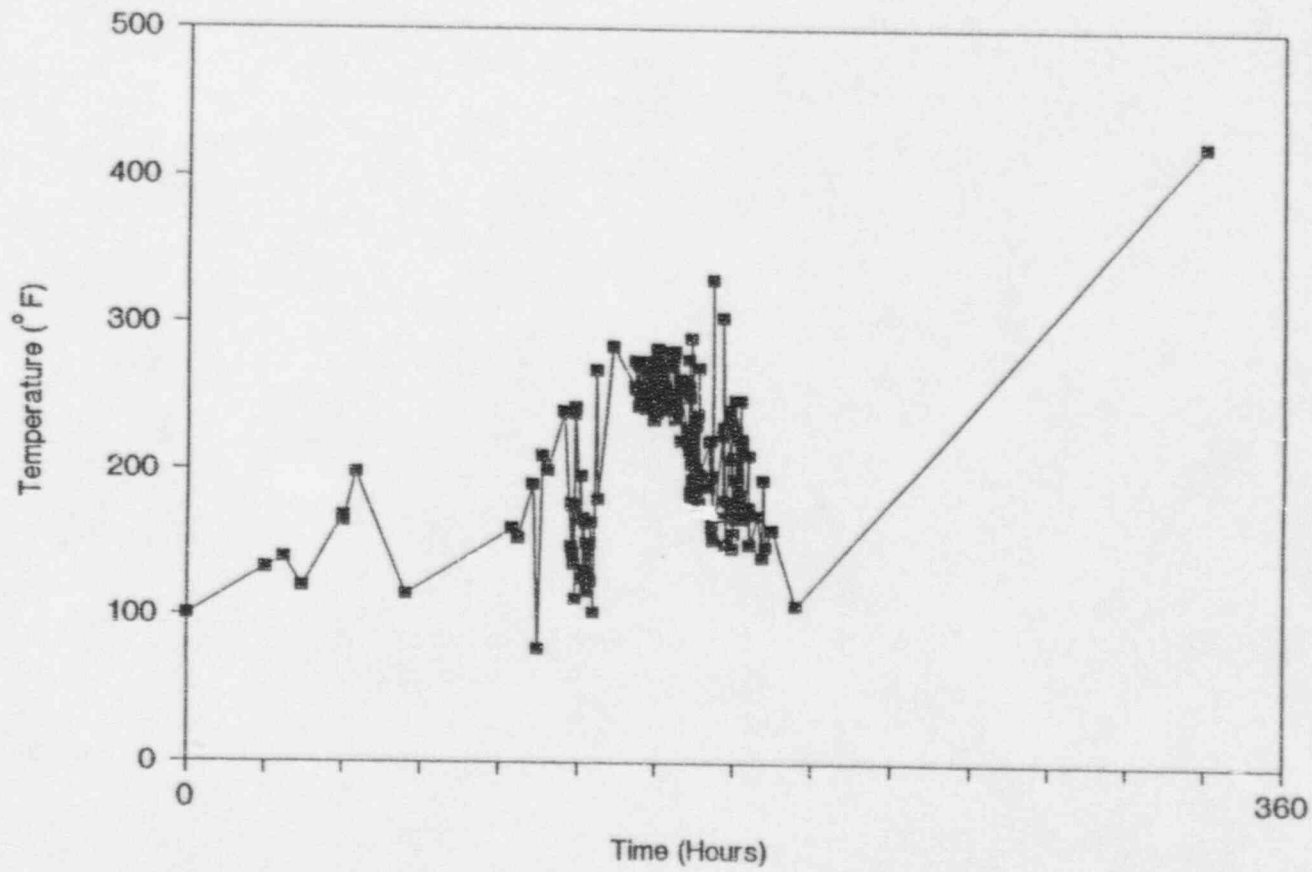


Figure 3-2. Temperature Cycling for Planned Shutdown of 1/23/88

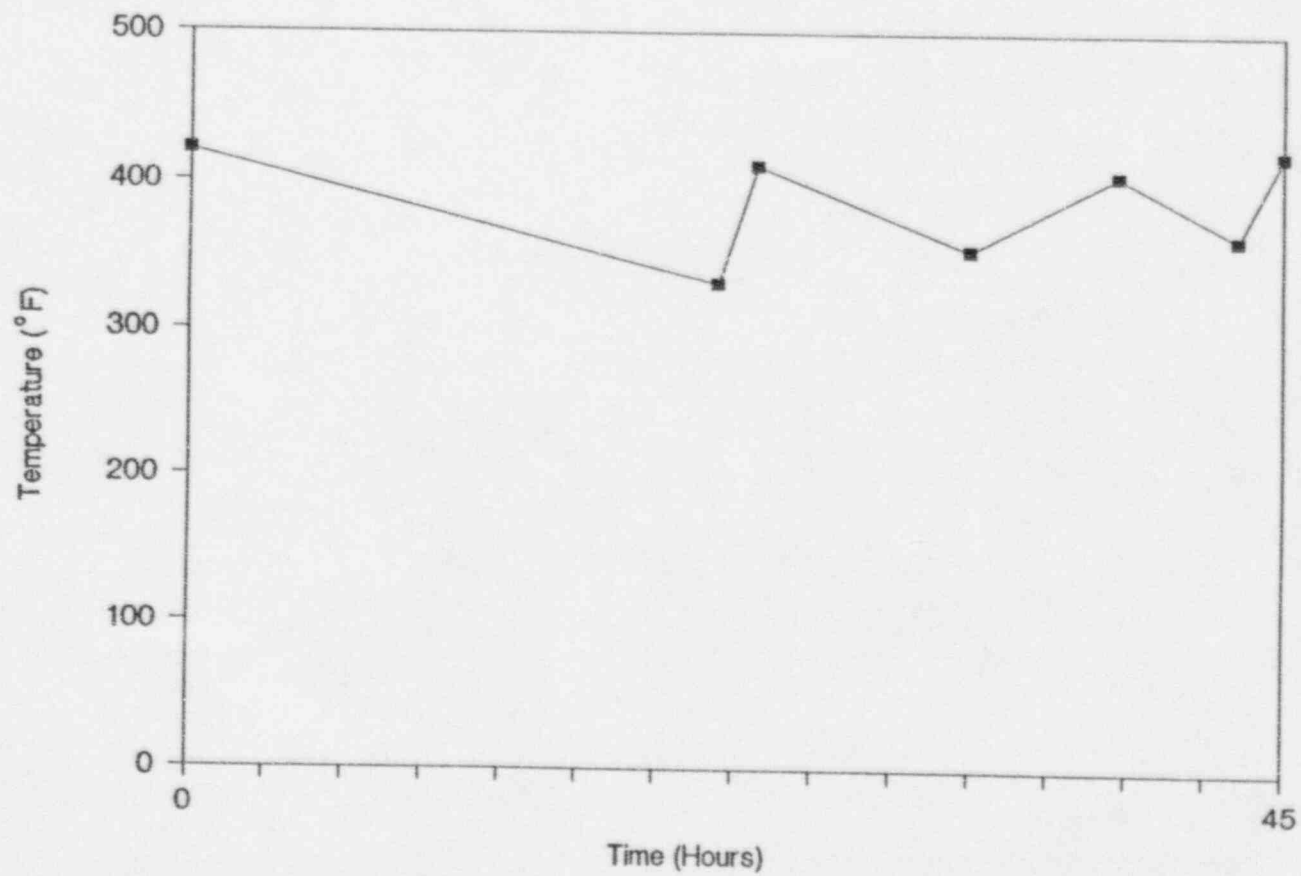


Figure 3-3. Temperature Cycling for 5/21/88 Maintenance Shutdown

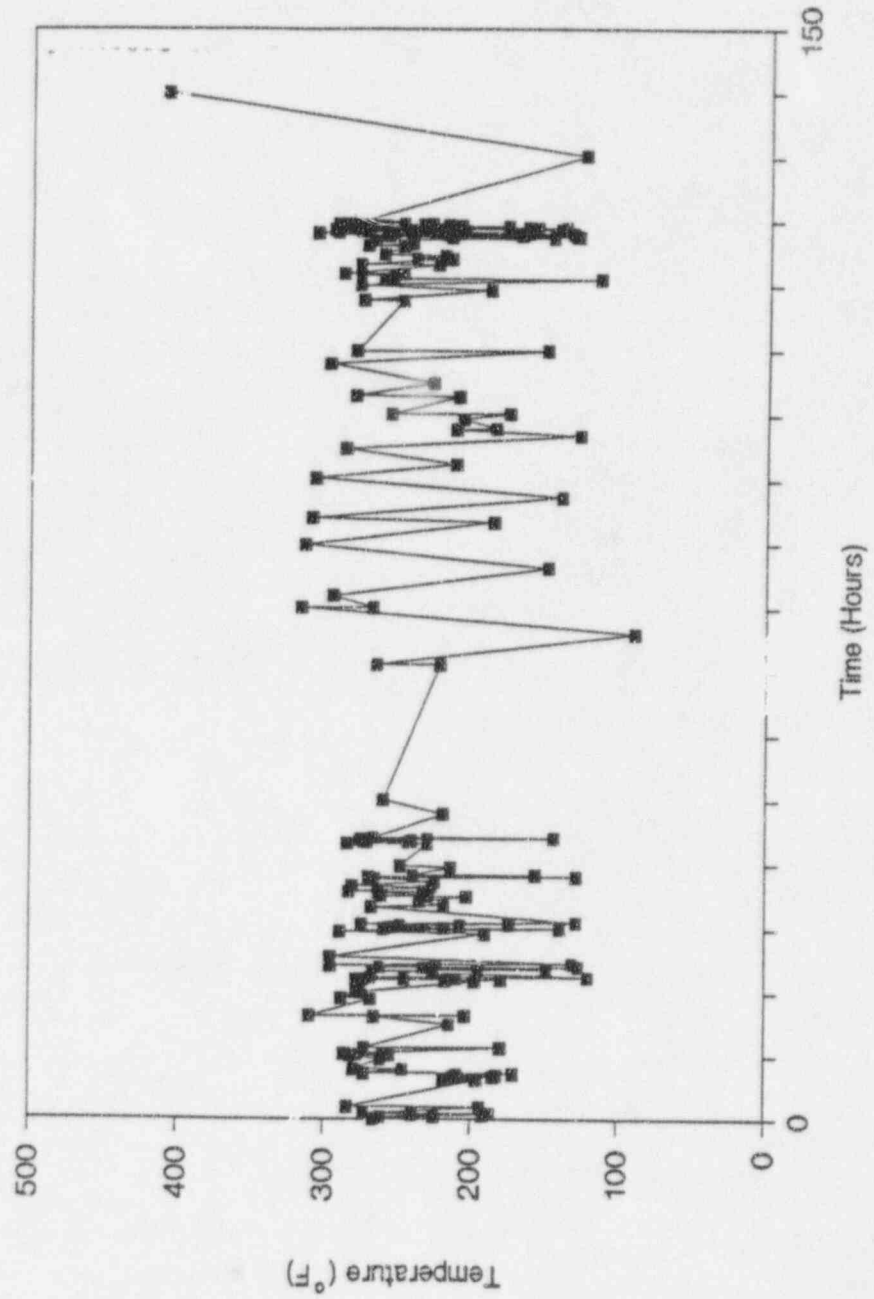


Figure 3-4. Temperature Cycling for 7/13/88 Forced Shutdown



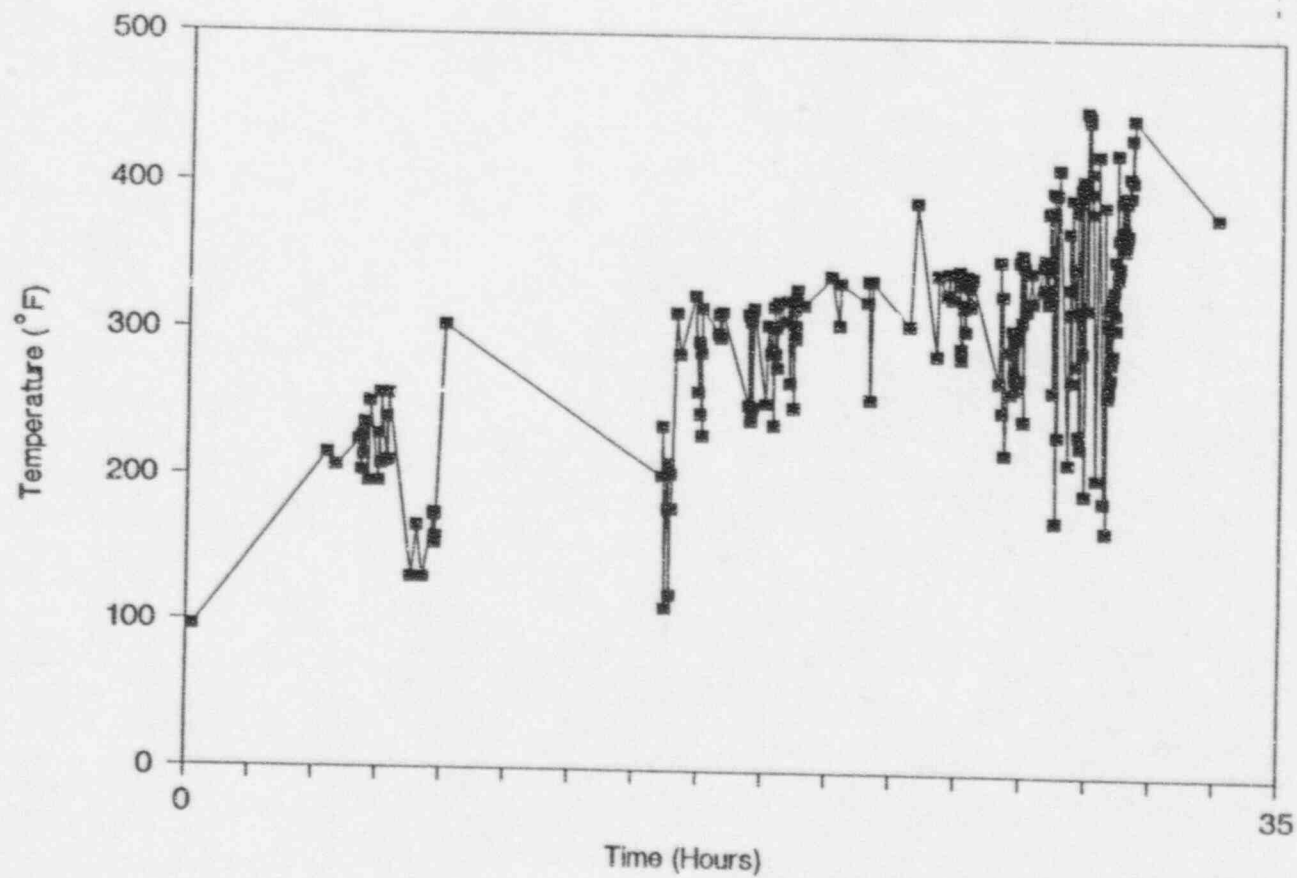


Figure 3-5. Temperature Cycling for 11/10/88 Refueling Shutdown

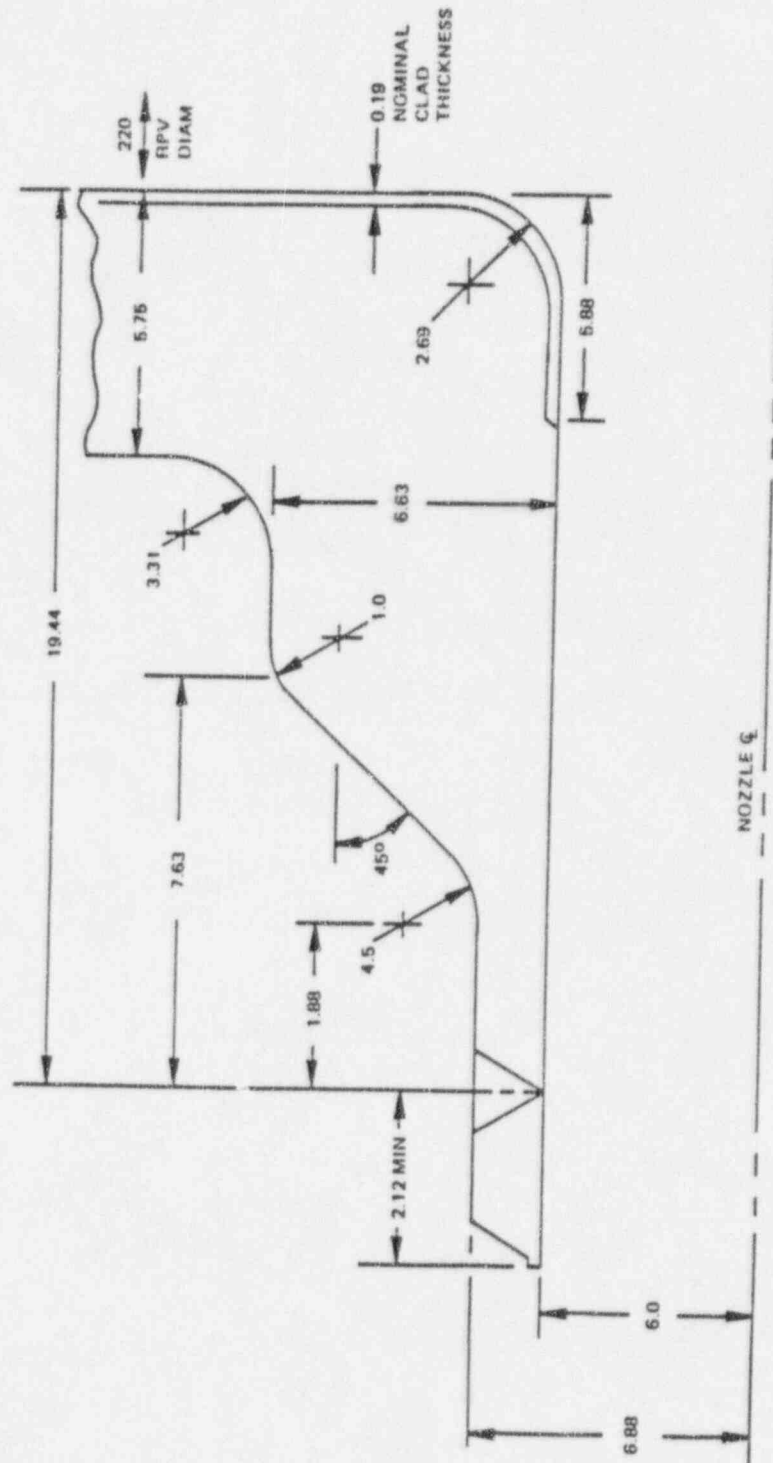
#### 4. THERMAL ANALYSIS

The finite element computer code ANSYS (Reference 6) was used to develop an axisymmetric model which simulated the Brunswick 1 feedwater nozzle. The isoparametric heat conduction element (STIF 55) was used. The model was developed using the nozzle configuration shown in Figure 4-1 (References 7 and 8). The same model with an isoparametric stress element was subsequently used for the stress analysis. Further discussion of the model configuration is included in Section 5.

The heat transfer coefficients and temperature boundary conditions were derived from Reference 9. The method of derivation is explained in the Appendix to this report. The use of annular temperatures and heat transfer coefficients removed the necessity of specifically modeling the thermal sleeve in the finite element analysis. The feedwater nozzle thermal sleeve design is a single sleeve welded to both the feedwater nozzle safe end and to the feedwater sparger. These heat transfer coefficients with the appropriate temperature boundary conditions are shown superimposed upon a drawing of the finite element model in Figure 4-2.

The initiation of feedwater flow was modeled by varying the temperatures in Zones 2 and 3 from 550°F down to the temperatures indicated in Figure 4-2, over a 3-sec interval. The temperatures were maintained at this level until steady-state conditions were reached. The 3-sec ramp was used rather than a step change, since it is conservative and still assures numerical stability in the computer solution.

The finite element model was regenerated and executed for the current analysis to assure identical results to those obtained previously in the original analysis.



NOTE: ALL DIMENSIONS ARE IN INCHES.

Figure 4-1. Nozzle Configuration

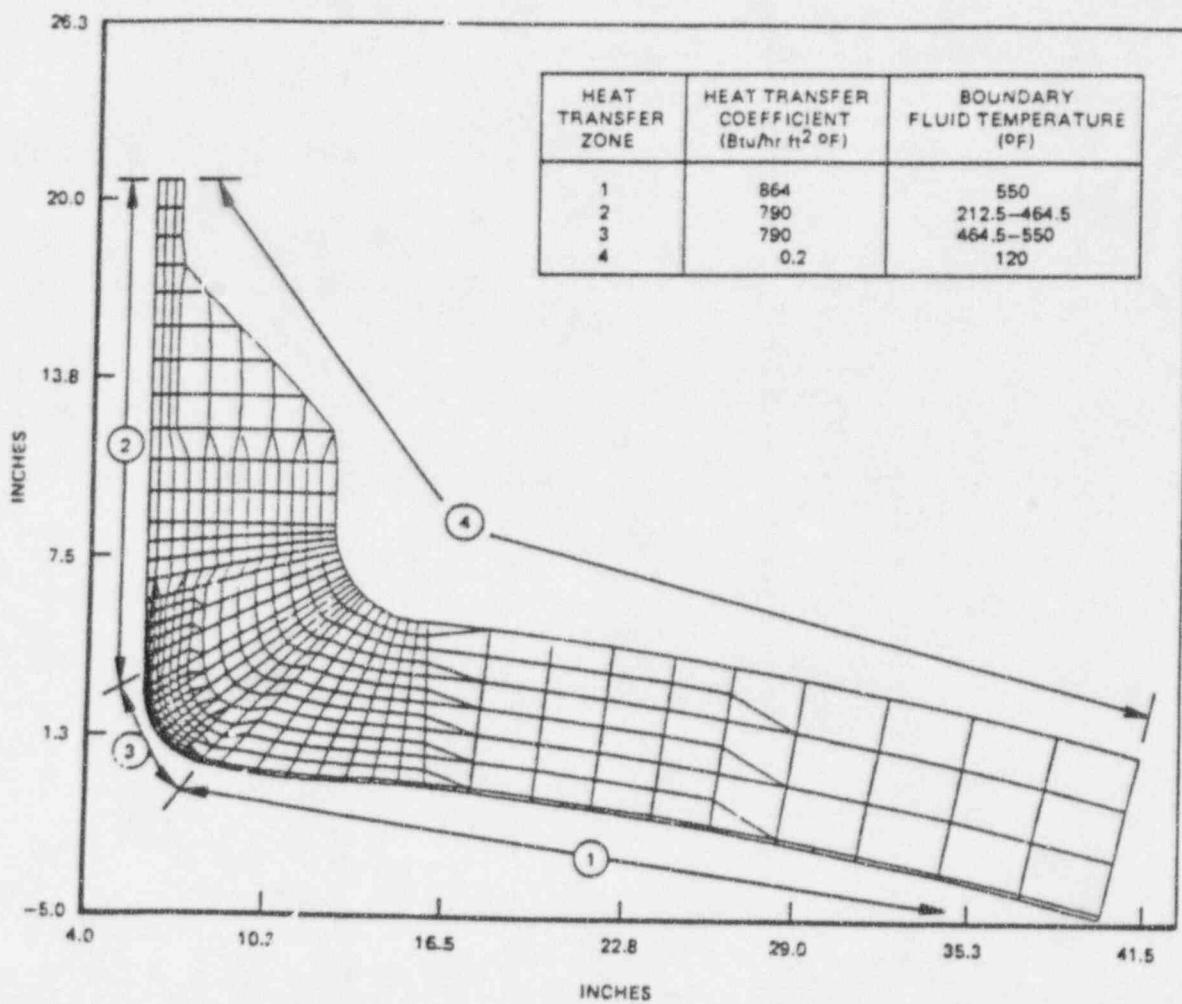


Figure 4-2. Thermal Boundary Conditions

## 5. THERMAL AND PRESSURE STRESSES

The results of the thermal analysis were applied to the previously mentioned finite element stress model to determine the thermal stresses. Iso-parametric stress elements (STIF 42) were used in the stress analysis. The nozzle was modeled by an axisymmetric finite element mesh with the vessel being represented as a spherical shell. This is a common approximation used in the stress analysis of a three-dimensional nozzle configuration in a cylindrical shell. This was adequate for thermal stresses, but pressure stresses required a scaling factor based on a three-dimensional analysis. The lengths of the nozzle safe end and pressure vessel section were each modeled to at least  $2.5 \sqrt{rt}$ , where  $r$  is the radius and  $t$  is the thickness of the nozzle. This was done to assure that end effects did not influence the stresses in the nozzle corner.

Thermal stresses were evaluated during several time intervals over the course of the transient by analyzing node pair temperature differences at various locations in the nozzle blend radius. Only the steady-state stresses and the stresses occurring at 4 minutes were used in the subsequent crack growth analysis, since they resulted in the most limiting stress profile in the nozzle blend radius region. The highest thermal stress occurs on the inside surface of the nozzle blend radius as shown in Table 5-1. The thermal stresses which developed from a  $\Delta T$  of 450°F are linearly scaled to the  $\Delta T$  described in the thermal cycle definitions (Section 3). The scaled thermal stresses are subsequently used in the crack growth analysis.

The maximum thermal stresses occurred in the stainless steel cladding area of the nozzle blend radius (ends at Element 337; Figure 5-1).

Pressure stresses for the case of a 1000-psi vessel pressure were also calculated; however, these stresses required application of a scaling factor. This was necessary because of the limitation of modeling a three-dimensional component with a two-dimensional axisymmetric model. Because the three-dimensional characteristics near the nozzle corner were not modeled, the peak

Table 5-1  
 SURFACE STRESSES TO CHOOSE MAXIMUM COMBINED STRESSES  
 (Steady State)

<u>Element</u>	<u>Thermal Hoop (psi)</u>	<u>Pressure Hoop (psi)</u>	<u>Pressure Ratioed to 1.5004 (psi)</u>	<u>Combined (psi)</u>
169	835	27196	40805	41640
185	491 <sup>o</sup>	28391	42597	47517
193	9178	29065	43609	52787
209	13412	29519	44290	57702
217	17395	29725*	44600*	61994
233	20809	29661	44503	65312
241	23795	29295	43954	67749
257	26598	28664	43007	69605
265	29168	27663	41506	70674
281	31721	26293	39450	71171*
289	33700	24462	36703	70403
305	35642	22808	34221	69863
313	37359	21232	31856	69215
329	39081*	19821	29739	68820
337	38874	18380	27577	66451
353	27304	16725	25094	52398
369	25130	14798	22203	47333

---

\*Maximum stress

Table 5-1

SURFACE STRESSES TO CHOOSE MAXIMUM COMBINED STRESSES (Continued)  
 (4 min after beginning of transient)

<u>Element</u>	<u>Thermal Hoop (psi)</u>	<u>Pressure Hoop (psi)</u>	<u>Pressure Ratioed to 1.5004 (psi)</u>	<u>Combined (psi)</u>
169	-2015	27196	40805	38790
185	2423	28391	42597	45021
193	7066	29065	43609	50675
209	12018	29519	44290	56308
217	16853	29725*	44600*	61452
233	21289	29661	44503	65792
241	25421	29295	43954	69375
257	29476	28664	43007	72483
265	33343	27663	41506	74849
281	37813	26293	39450	77263
289	41970	24462	36703	78673
305	45883	22808	34221	80104
313	49460	21232	31856	81316
329	53070	19821	29739	82809*
337	54279*	18380	27577	81856
353	46090	16725	25094	71184
369	45903	14798	22203	68106

---

\*Maximum stress

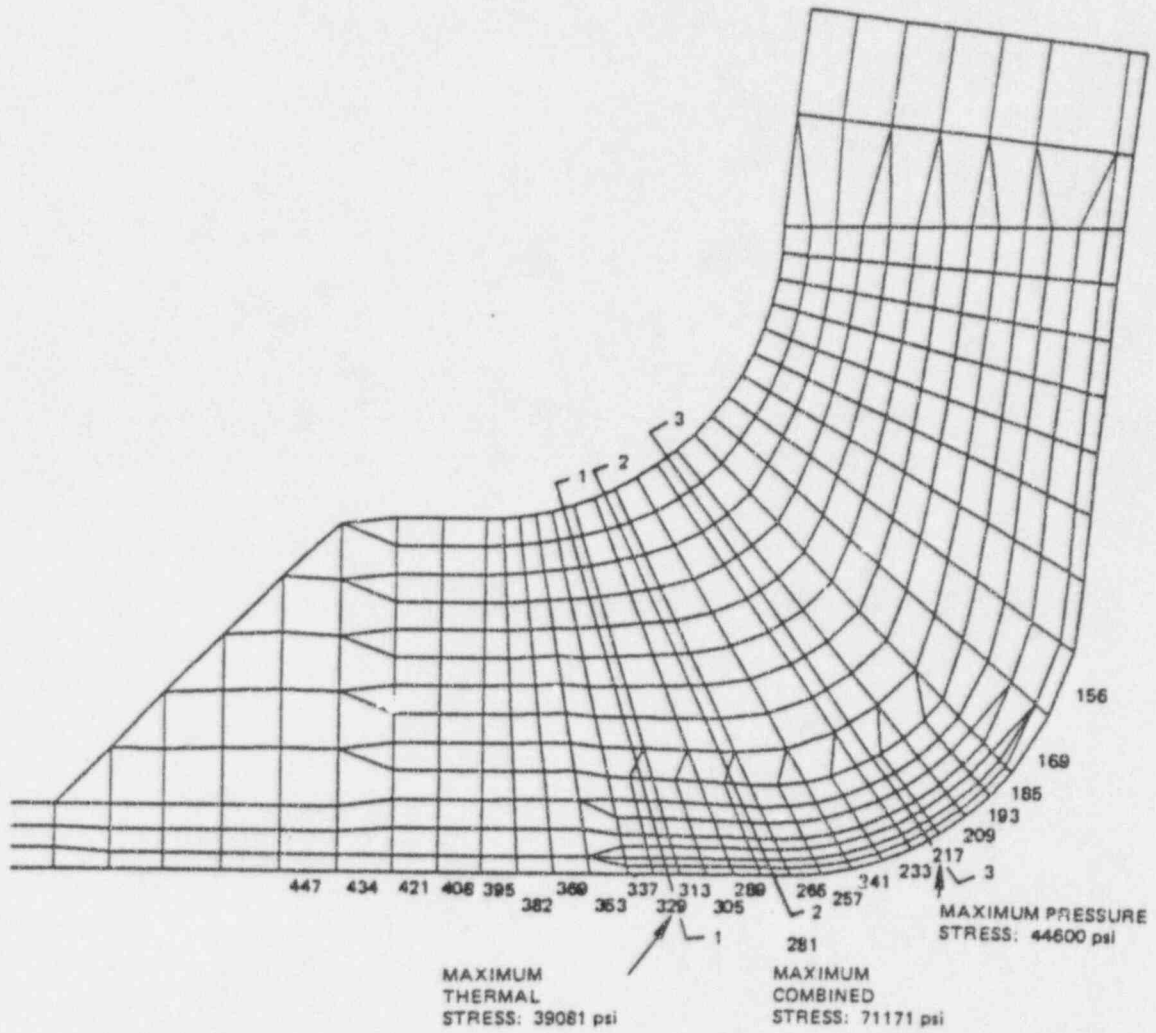


Figure 5-1. Feedwater Nozzle-Brunswick 1 Location of Maximum Surface Stress (Steady State)



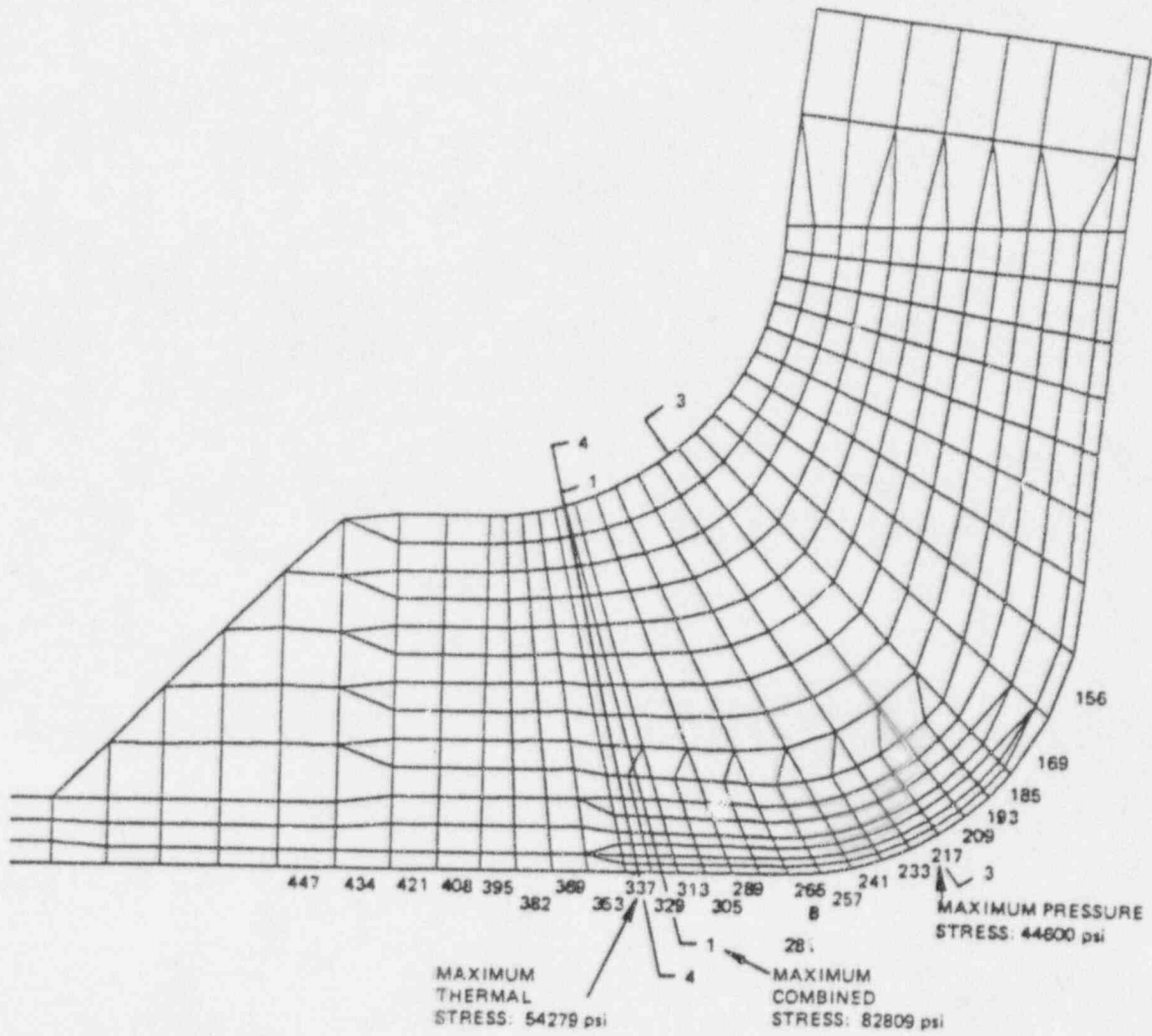


Figure 5-2. Feedwater Nozzle-Brunswick 1 Location of Maximum Surface Stress (Transient  $t = 4$  minutes)

stresses at the nozzle corner were not accounted for accurately. Therefore, a generic three-dimensional model developed by Gilman and Rashid (Reference 10) was used to scale the pressure stress. The scaling factor for the pressure stress is given by the ratio of the peak pressure stress on the inside surface reported by Gilman and Rashid to the peak pressure stress on the inside surface from the finite element model used in this report. The peak pressure stress of the finite element model was 29,725 psi, while the peak pressure stress reported by Gilman and Rashid is 44,600 psi. This resulted in a scaling factor of 1.5004. The scaled peak pressure stress on the inside surface is shown in Figure 5-1.

The combined thermal and scaled peak pressure stresses were examined to determine the area where the combined peak stress on the inside surface occurs, as shown in Table 5-1. The stresses at the cross section associated with the limiting stress profile (see Table 5-2, and cross section 4-4 on Figure 5-2) were used to calculate crack growth.

Table 5-2  
LIMITING STRESS PROFILE (CROSS SECTION 4-4)

<u>Distance from Inside Surface - (in.)</u>	<u>Pressure Hoop Ratioed to 1.5004 (psi)</u>	<u>Thermal Hoop 4 minutes (psi)</u>
0.0	27577	54279
0.074	27028	52036
0.229	26325	35698
0.397	25241	32438
0.596	24161	29058
0.846	23049	24536
1.147	21849	20309
1.501	20587	15354
1.886	19843	12675*
2.336	18252	10057
3.004	16570	7723
3.632	15084	5688
4.251	13705	3878
4.882	12360	2227
5.501	10975	669

\*Steady-state thermal stresses were used from point "\*" to the outside surface of the nozzle because the steady-state thermal stresses result in greater crack growth.

## 6. CRACK GROWTH ANALYSIS

## 6.1 STRESS INTENSITY FACTOR CALCULATIONS

Stress intensity factors were determined using solutions for standard stress distributions (e.g., constant, linear, quadratic, and cubic variations) and applying the superposition principle. The stress intensity solution for these unit load cases was expressed in terms of the crack length and appropriate magnification factors for the specific crack geometry (Figure 6-1). The stress intensity for an arbitrary stress distribution was then obtained by fitting a third-order polynomial of the form:

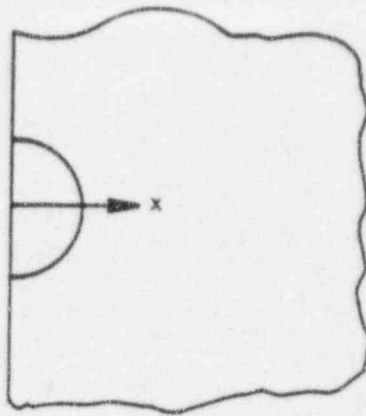
$$\sigma = A_0 + A_1X + A_2X^2 + A_3X^3$$

and applying the principle of superposition. Once the curve fit parameters  $A_0$ ,  $A_1$ ,  $A_2$ , and  $A_3$  were known, the stress intensity factor was determined as a function of crack depth using the equations in Figure 6-1.

Magnification factors for several common two-dimensional geometries are available in References 11 and 12. For the feedwater nozzle, a set of three-dimensional magnification factors is presented in Reference 1. As illustrated in Figure 6-1, the nozzle corner factors (0.706, 0.537, 0.448, and 0.393) were obtained by averaging the magnification factors developed for circular surface crack geometries in half and quarter spaces. This expression (labeled FUN 11) was used to calculate stress intensity factors in the fracture mechanics evaluation which follows.

The pressure and thermal stress distributions were fit to third-order polynomials using a standard least squares procedure. Overall accuracy of the polynomial representations is considered more than adequate.

Substituting these polynomial coefficients ( $A_0$ ,  $A_1$ ,  $A_2$  and  $A_3$ ) into the FUN 11 stress intensity factor expression of Figure 6-1 leads to the stress intensity factor versus crack depth data shown in Figures 6-2 and 6-3. (These stress intensity factors apply to cross section 4-4.)



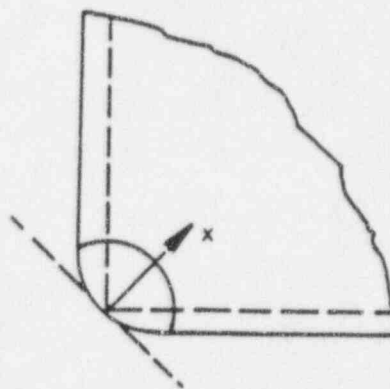
FUN 9 - SEMI-CIRCULAR CRACK IN HALF-SPACE

$$K_I = \sqrt{\pi a} [0.688 A_0 + 0.522 (2a/\pi) A_1 + 0.434 (a^2/2) A_2 + 0.377 (4a^3/3\pi) A_3]$$



FUN 10 - QUARTER-CIRCULAR CRACK IN QUARTER-SPACE

$$K_I = \sqrt{\pi a} [0.723 A_0 + 0.551 (2a/\pi) A_1 + 0.462 (a^2/2) A_2 + 0.408 (4a^3/3\pi) A_3]$$



FUN 11 - SIMULATED 3-D NOZZLE CORNER CRACK

$$K_I = \sqrt{\pi a} [0.706 A_0 + 0.537 (2a/\pi) A_1 + 0.448 (a^2/2) A_2 + 0.393 (4a^3/3\pi) A_3]$$

Figure 6-1. Boundary Integral Equation/Influence Function Magnification Factors for BWR Feedwater Nozzle

6-3

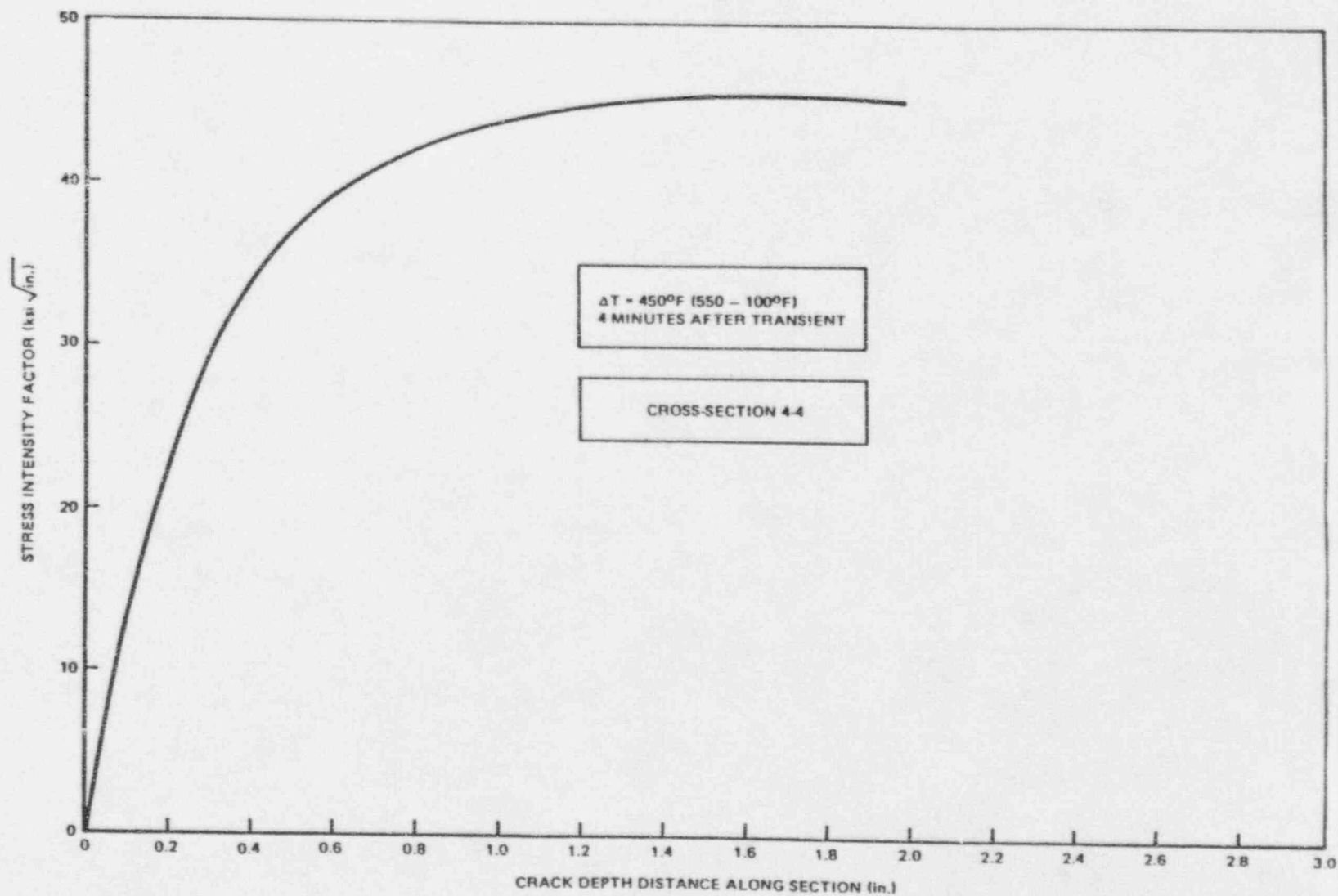


Figure 6-2. Stress Intensity Factor versus Crack Depth (Thermal Stresses, 4 minutes)

6-9

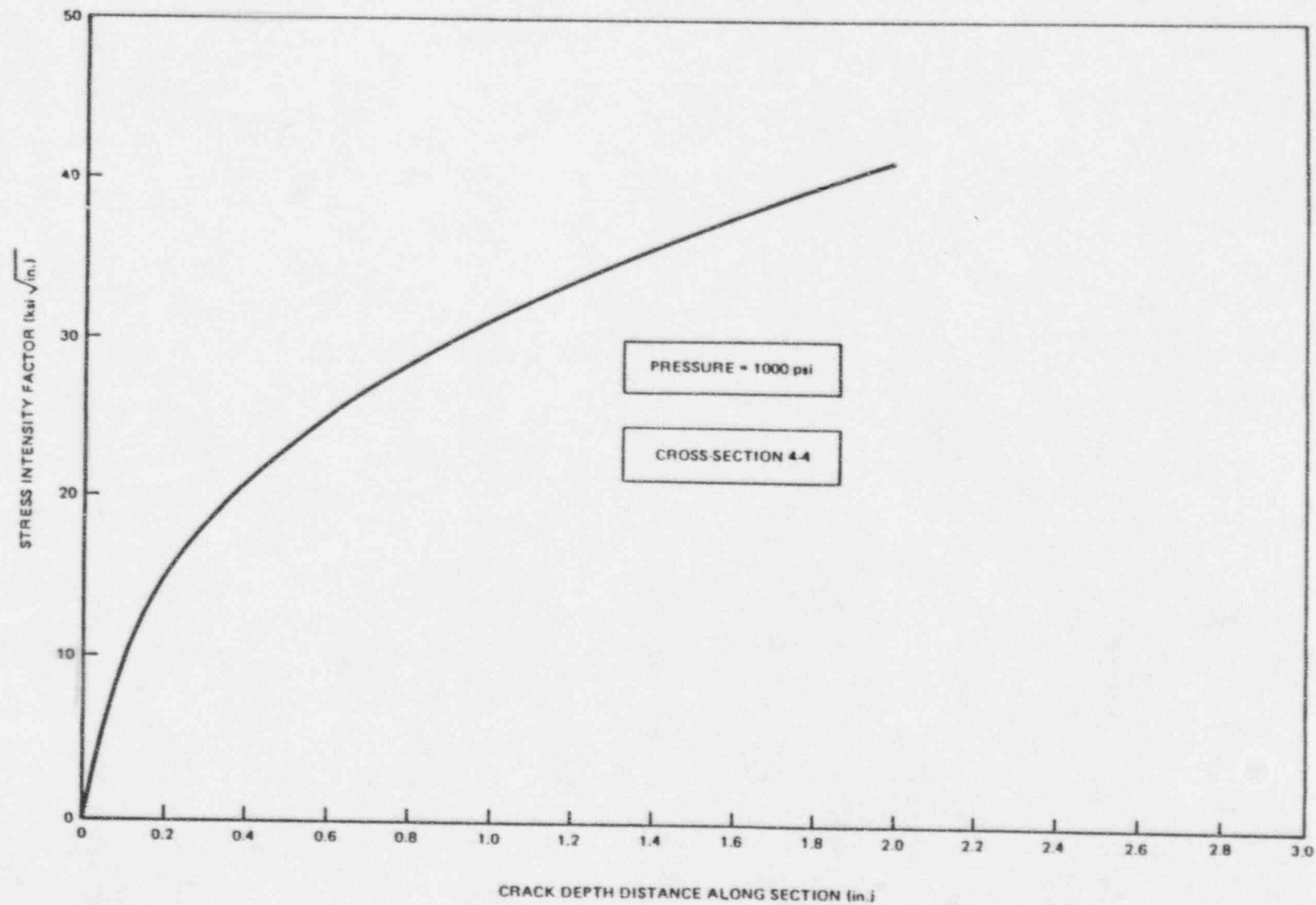


Figure 6-3. Stress Intensity Factor versus Crack Depth (Pressure Stresses)

## 6.2 CRACK GROWTH DATA

Figure 6-4 represents the fatigue crack growth data for low alloy steel from Section XI of the ASME Code (Reference 13). The R-ratio ( $K_{min}/K_{max}$ ) dependence of this data is built-in by representing three cases: (1) R-ratio less than 0.25, (2) R-ratio between 0.25 and 0.65, and (3) R-ratio greater than 0.65. These data were used to determine the growth of an assumed 0.25-inch initial depth crack.

The best-fit compilation of fatigue crack growth data used in the original revision of this report was not used in the current analysis. That relationship is not valid for high values of R-ratio. Much of the data obtained for Brunswick 1 yielded high R-ratios ( $>0.9$ ). As a result, unrealistic crack growth would result from the use of this relationship.

## 6.3 CRACK GROWTH EVALUATION

The thermal cycle definitions are represented by Figures 3-1 through 3-5 for startup/shutdown and scram/return to full power events. A projected total of 163 startup/shutdown events and 323 scram events was made for Brunswick 1 over the 40-year design life of the plant as described in Section 3.

The analysis conservatively assumed that the initial crack depth of 0.25 inch included the cladding thickness. Since the thermal stresses are higher in the stainless steel cladding region, the corresponding stress intensity factor would also be greater, thereby resulting in a more rapid crack growth propagation.

The procedure for calculating the crack propagation is as follows: For each cycle, the maximum and minimum stress and the number of occurrences were calculated. From this, the stress intensity factor range and corresponding R-ratio were calculated for the cycle being analyzed. Using this and the selected crack growth relationship, the incremental crack growth was



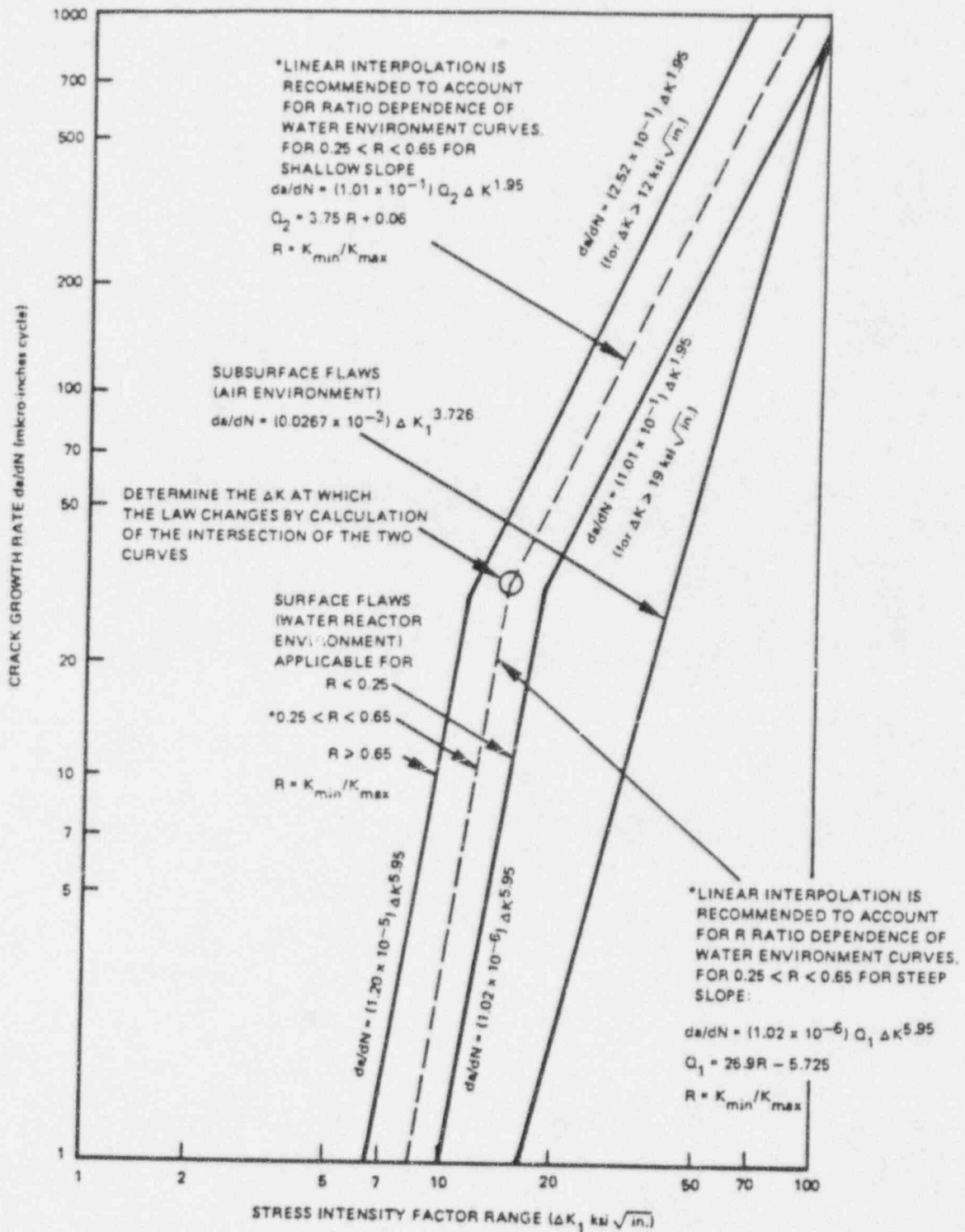


Figure 6-4. Reference Fatigue Crack Growth Curves for Carbon and Low Alloy Ferritic Steels

calculated for that event. The crack size was updated and the procedure repeated. This continued for every cycle until the entire life was analyzed.

The pattern of events was assumed to be:

41 sets of: 4 startup/shutdown events followed by  
8 scram/return to full power events  
(Figure 3-1).

Note that  $41 \times 4 = 164$  startups and  $41 \times 8 = 328$  scrams. The effects of modeling five extra scram events and one extra startup/shutdown event, although conservative, is considered small.

The four startup/shutdown events were further broken down as follows:

- 1 1/23/88 Planned Shutdown event (Figure 3-2)  
(including the mirror-image startup)
- 1 5/21/88 Maintenance Shutdown event (Figure 3-3)  
(including the mirror-image startup)
- 1 7/23/88 Forced Shutdown event (Figure 3-4)  
(including the mirror-image startup)
- 1 11/10/88 Refueling Shutdown event (Figure 3-5)  
(including the mirror-image startup)

---

Total = 4

One crack propagation calculation was made corresponding to the limiting stress profile shown in Table 5-2.

## 7. RESULTS AND CONCLUSIONS

Because of the recent acquisition of plant-unique data, the feedwater nozzle thermal cycle definitions defined in Section 3 were assumed to be representative of all startup/shutdown and scram events. The number of events over the plant life as projected using plant-specific data (References 2, 3 and 4) was utilized. A plant-specific finite element stress analysis was performed for the feedwater nozzle.

The fracture mechanics analysis was based on the thermal stresses obtained from the finite element analysis, the thermal cycle definitions derived from actual plant feedwater data, and the historical frequency of the number of startup/shutdown and scram/return to service events.

The results of the fracture mechanics analysis are given in Figure 7-1 for the limiting location (cross section 4-4) as a function of the number of years since initial plant startup.

Using the 1989 ASME Section XI fatigue crack growth curves, the analysis shows that the postulated 0.25-in. crack becomes 0.56 inch deep after the 40-year plant design life.

The operating history used in the current analysis was based on an extrapolation of the initial twelve years of plant operation. Because of "learning curve" effects which are typically experienced by operating reactors during their initial years of operation, this extrapolation is most likely conservative (as recognized by the large number of startup/shutdown events). Based on this extrapolation and the utilization of temperature magnitudes considered typical for Brunswick 1 operation, this re-evaluation demonstrates full compliance with the requirements of NUREG-0619. Periodic examinations, as required by NUREG-0619, can provide additional justification of these analytical results.

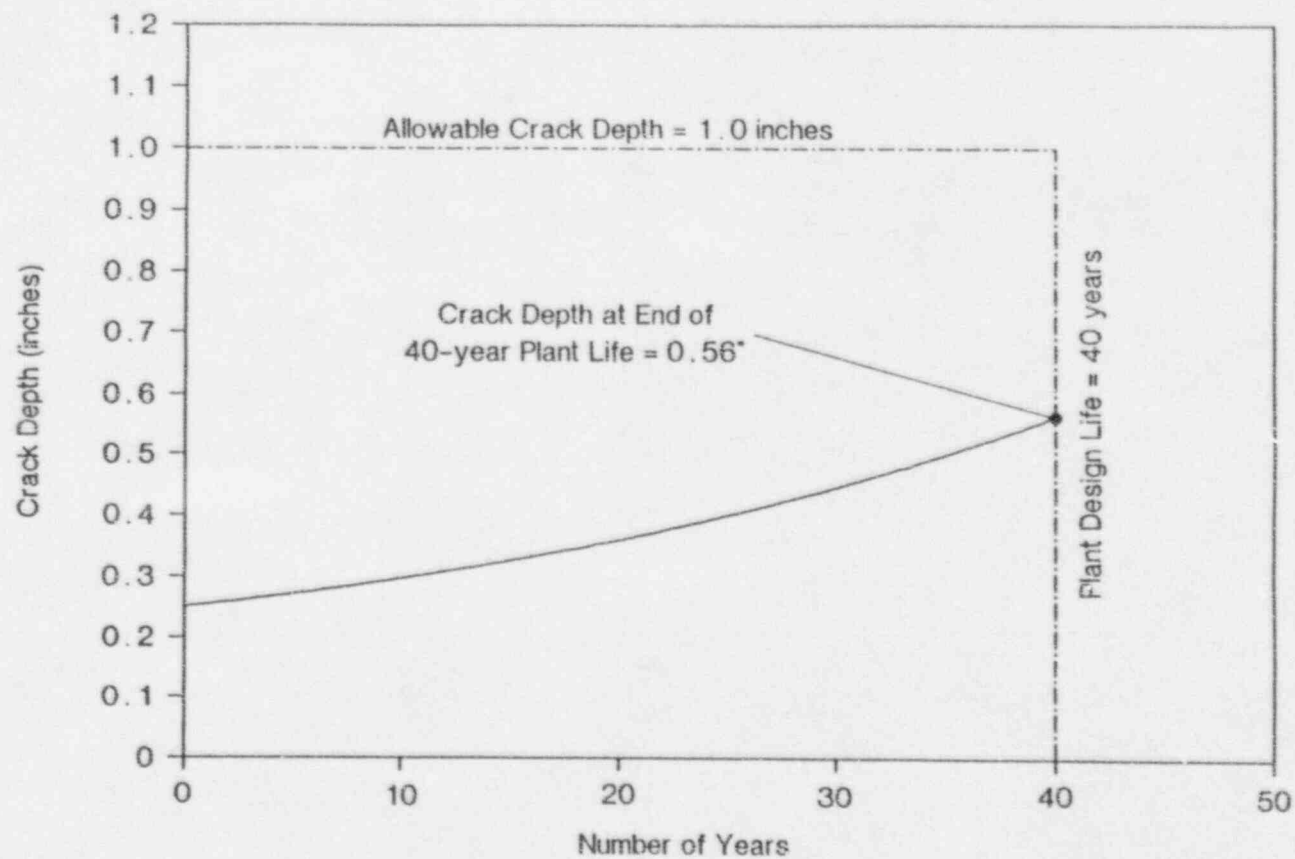


Figure 7-1. Crack Depth versus Number of Years

# 8. REFERENCES

1. NEDE-21821-A, "Boiling Water Reactor Feedwater Nozzle/Sparger Final Report," General Electric Company, August 1979.
2. Letter EGE-146, File BG0029A-AA-A500, J. M. Brown (CP&L) to G. L. Stevens (GE), "Brunswick Steam Electric Plant, Unit Nos. 1 & 2 NUREG-0619 Analyses, PCN G00029A Information Transmittal," November 17, 1989.
3. NEDO-22196, "Reactor Pressure Vessel Thermal Cycle Fatigue Evaluation for Brunswick Steam Electric Plant Units 1 and 2," General Electric Company, March 1983.
4. Letter EGE-164, File BG0029A-AA-A500, A. M. Lucas (CP&L) to G. L. Stevens (GE), "Carolina Power & Light Company, Brunswick Steam Electric Plant Units 1 & 2, Feedwater Nozzle NUREG-0619 Crack Growth Analysis Update," December 10, 1990.
5. GE Services Information Letter (SIL) Number 318, "BWR Reactor Vessel Cyclic Duty Monitoring," December 1979.
6. G. J. DeSalvo and J. A. Swanson, "ANSYS Engineering Analysis System User's Manual," Swanson Analysis Systems, Inc., May 1, 1989, Revision 4.4.
7. GE Drawing 767E723, Rev. 1, "Feedwater Nozzle Safe End," July 1975.
8. Chicago Bridge and Iron Drawing Number 31, Rev 17, "12-In. Diameter Feedwater Nozzles," October 1971.
9. NEDE-21659-1, C. M. Kwong and H. Choe, "Moss Landing Feedwater Nozzle/Sparger Test Data Files," February 1979.
10. J. D. Gilman and Y. R. Rashid, "Three-Dimensional Analysis of Reactor Pressure Vessel Nozzles," Proc. 1st Int. Conf. on Structural Mechanics in Reactor Technology, Vol. 4 Part G, September 1971.
11. ASTM-STP-590, C. B. Buchalet and W. H. Bamford, "Stress Intensity Factor Solutions for Continuous Surface Flaws in Reactor Pressure Vessels," Mechanics of Crack Growth, American Society for Testing and Materials, 1975.
12. ASTM-STP-590, R. Labbens, A. Pellissier-Tanon and J. Heliot, "Practical Method for Calculating Stress Intensity Factors Through Weight Functions," Mechanics of Crack Growth, American Society for Testing and Materials, 1975.
13. ASME Boiler and Pressure Vessel Code, Section XI, 1989 Edition.
14. NSEO-75-882, "Effects of Reactor Water Cleanup Reroute on Feedwater Nozzle Fatigue Usage, Brunswick Steam Electric Plant Units 1 and 2," August 1982.

# APPENDIX

## THERMAL BOUNDARY CONDITIONS

### A.1 HEAT TRANSFER COEFFICIENTS

The annular heat transfer coefficients were developed from the data of Reference A-1 as follows. The data base consisted of four tests which were run at low feedwater flow and zero leakage flow. The heat transfer coefficients during the tests were determined from eight heat flux meters mounted circumferentially around a section of the nozzle blend radius.

The highest heat transfer coefficient measured was taken and corrected to account for the difference in nozzle blend radius between the test sparger and the Brunswick 1 sparger. The Nusselt number,  $Nu$ , is proportional to the Reynolds number to the  $n$ th power, where  $n$  is typically 0.8. The Reynolds number is in turn directly proportional to the nozzle blend radius,  $R$ . Therefore, the Nusselt number is proportional to the nozzle blend radius raised to the 0.8 power. In equation form,

$$Nu \propto R^{0.8}$$

The heat transfer coefficient,  $h$ , is given by

$$h = Nu (k/R)$$

where  $k$  is the thermal conductivity of the fluid. Thus

$$h \propto R^{-0.2}$$

This proportionality is used to correct the heat transfer coefficient. In the tests of Reference A-1,  $h = 840 \text{ Btu/hr-ft}^2\text{-}^\circ\text{F}$  and  $R = 2$  inches. For the Brunswick 1 sparger,  $R = 2.69$  inches. Therefore,  $h = 790 \text{ Btu/hr-ft}^2\text{-}^\circ\text{F}$ .

## A.2 BOUNDARY TEMPERATURE CONDITION

Boundary (or annulus) temperatures were taken from the aforementioned four tests. The fourth test was not used because of the abnormally high percentage of steam carryunder. The test data is expressed in terms of a normalized temperature which is equal to the difference of the annular fluid temperature and the feedwater temperature divided by the difference of the reactor temperature and the feedwater temperature. Readings are available at several circumferential locations at four sections of the nozzle. At each section, the lowest readings for each test were averaged to produce the final result.

The annulus fluid temperatures, as determined from these Moss Landing tests, are given in Table A-1 as a function of position of the welded sleeve nozzle configuration. The expression for obtaining the annulus fluid temperature is as follows:

$$T = T_{FW} + C_1 (T_V - T_{FW})$$

where

- T = annulus fluid temperature (°F)
- $T_{FW}$  = feedwater temperature (°F)
- $T_V$  = vessel temperature (°F)
- $C_1$  = coefficient from Table A-1

## A.3 REFERENCE

- A.1 NEDE-21659-1, C. M. Kwong and H. Choe, "Moss Landing Feedwater Nozzle/Sparger Test Data Files," February 1979.



Table A-1  
C<sub>1</sub> COEFFICIENT  
(GE Proprietary)

<u>Location</u>	<u>C<sub>1</sub></u>
F2	0.225
A	0.25
B	0.54
C	0.81

Use linear interpolation between locations as illustrated in Figure A-1.



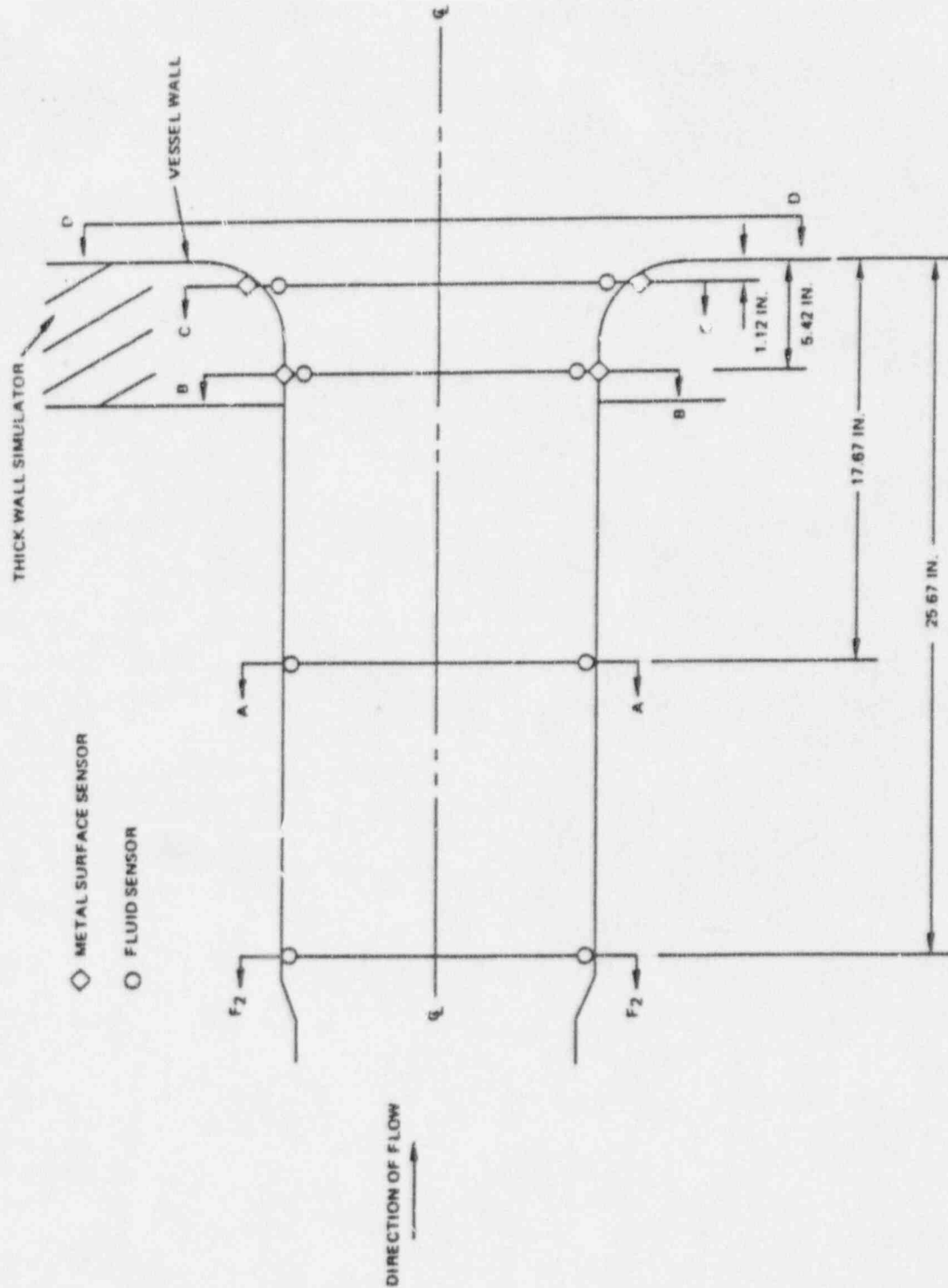


Figure A-1. Instrumentation of Feedwater Nozzle and Vessel Wall  
(from Moss Landing Tests, Reference A-1)

## DISTRIBUTION

<u>Name</u>	<u>M/C</u>
K. F. Cornwell	732
S. Ranganath	747
W. Yee	BRU
A. D. Ketcham	BRU
G. L. Stevens (15)	747
GE-NE Library (2)	528